

Precise measurement of cerebral blood flow in newborn piglets from the bolus passage of indocyanine green

R Springett^{1,3}, Y Sakata² and D T Delpy¹

¹ Department of Medical Physics and Bioengineering, University College London, London WC1E 6JA, UK

² Department of Paediatrics, University College London, London WC1E 6JA, UK

E-mail: rspringett@medphys.ucl.ac.uk

Received 7 March 2001

Published 19 July 2001

Online at stacks.iop.org/PMB/46/2209

Abstract

Indocyanine green (ICG) is a near-infrared dye that has the potential to be used as a tracer for the minimally invasive measurement of cerebral blood flow (CBF). In order to examine the technique, the arterial and cerebral concentrations of ICG were measured in newborn piglets during the bolus passage of ICG at normocapnia and two levels of mild hypercapnia. The results were analysed by applying the Fick principle in both integral and differential forms using a linear regression technique to improve the precision of calculated values of CBF.

It was found that the integral method, which has been used previously, is particularly sensitive to errors in the time registration between the arterial and tissue signals whereas the differential method is less so. In addition, the differential method allows the venous outflow to be calculated which gives further information on the state of the capillary bed. CBF was 39.7 ± 4.6 ml 100 g⁻¹ min⁻¹ at an arterial carbon dioxide tension (P_{aCO_2}) of 33.0 ± 2.2 mmHg and increased to 53.7 ± 9.1 and 75.4 ± 15.2 ml 100 g⁻¹ min⁻¹ at a P_{aCO_2} of 42.1 ± 2.6 and 54.2 ± 3.1 mmHg respectively (mean \pm SD, $n = 7$). There was no significant change in cerebral metabolic rate for oxygen, validating the value of blood flow to an arbitrary scaling factor. When the inspired CO₂ fraction was returned to zero, calculated CBF returned to baseline with a variation of 7% of the mean, indicating that this technique is highly precise.

³ Address for correspondence: Department of Medical Physics and Bioengineering, University College London, Shropshire House, 11–20 Capper Street, London WC1E 6JA, UK.

1. Introduction

Indocyanine green (ICG) is a near-infrared (NIR) dye that has the potential to be used as a tracer for the minimally invasive measurement of cerebral blood flow. Once injected as a bolus, it rapidly binds to plasma albumin and is not expected to cross the blood–brain barrier. The tissue concentration of the dye can then be related to the arterial and venous concentrations using the Fick principle, which states that the quantity of a non-diffusible tracer within the tissue is equal to the accumulation of the difference between the arterial inflow and the venous outflow of the tracer. The Fick principle can be expressed in integral form as

$$C_t(t) = F \int^t (C_a(t) - C_v(t)) dt \quad (1)$$

where $C_t(t)$ is the tissue concentration, F is the blood flow, $C_a(t)$ is the arterial concentration of the dye and $C_v(t)$ is the venous concentration of the dye. The inflow of the dye into the tissue is the product of flow and arterial concentration and the outflow is the product of flow and venous concentration. If the measurement is made within the minimum transit of the tissue then $C_v(t)$ can be assumed to be zero and only the tissue and arterial concentration are required to produce a measurement of blood flow. Commercial instruments are available which measure the arterial concentration from either an indwelling catheter (Pulsion Medical Systems, Munich, Germany) or from pulse oximetry (Nihon Koden, Tokyo, Japan) and the tissue concentration can be measured using near-infrared spectroscopy.

If the arterial input function is not known then an absolute value of blood flow cannot be measured and only a blood flow index can be calculated (Kuebler *et al* 1998). If the arterial function is known, the blood flow can be calculated using equation (1) from a linear regression between the numerically integrated arterial curve on the x -axis and the tissue curve on the y -axis (see figure 3(b)). The blood flow is then given by the gradient of a regression line. Previous analysis of ICG bolus transits has calculated blood flow from the ratio of tissue concentration to integrated arterial concentration evaluated at a single time point (Patel *et al* 1998, Roberts *et al* 1998) and this is equivalent to the gradient between the baseline and a single point on the regression curve. The advantage of the regression technique is that all the data from the tissue concentration curve contribute to the calculated value of blood flow, which is therefore more robust with respect to noise on the signal. In addition, with this method it is easy to time-register the tissue and arterial signals and to determine the minimum transit time without recourse to statistical methods (Elwell *et al* 1997).

The Fick principle can also be expressed in differential form as

$$C'_t(t) = \frac{dC_t(t)}{dt} = F(C_a(t) - C_v(t)) \quad (2)$$

and blood flow can be calculated similarly from a linear regression between $C'_t(t)$ and $C_a(t)$. Although numerical differentiation is a noise-amplifying process and can only be performed if the data have a high signal to noise ratio, this method has the advantage that the venous outflow can be determined once flow has been calculated from the early part of the regression (when $C_v(t)$ is zero) and so provides further information on the state of the vasculature. In addition, it will be shown that this method provides a value of blood flow that is more robust with respect to errors in time-registration between the tissue and arterial curves.

Although fast acquisition is possible using computed tomography (CT) and magnetic resonance imaging (MRI), in general the time resolution is not sufficient to use the Fick principle and algorithms are employed which measure cerebral blood volume and mean transit time. Blood flow is then calculated using the central volume principle. In contrast to the algorithms applied in this paper, the approximation that the tissue concentration is equivalent

to the outflow which is used to calculate mean transit time is inexact and has been criticized previously (Lassen 1984, Weisskoff *et al* 1993).

The correctness of a measurement technique can be described by its accuracy, defined as the ability to reproduce the value determined by a gold standard, and its precision defined as the ability to measure small changes. For instance, a technique with a poor signal to noise could have a high accuracy because the mean value of many measurements could reproduce the true value, but a poor precision because there is a large variation in each individual measurement. The aim of this paper is to examine the ICG bolus technique together with a rapid near-infrared spectroscopic measurement of the tissue concentration in a newborn piglet model in order to determine the necessary conditions for the precise measurement of cerebral blood flow. Combining a value of CBF with arterial and sagittal sinus blood samples allows the cerebral metabolic rate for oxygen (CMRO₂) to be calculated. By showing that this blood flow technique reproduces the previous finding that hypercapnia causes a large increase in CBF but no change in CMRO₂ (Siesjo 1978), it is possible to validate the accuracy of the blood flow value to an arbitrary scaling factor.

2. Methods

Seven piglets, born at term but less than 24 h old and weighing 1.80 ± 0.25 kg (mean \pm SD), were sedated with midazolam and anaesthetized with 2% isoflurane. A tracheotomy was performed and the piglets were artificially ventilated with an intermittent positive pressure ventilator using an oxygen and nitrogen gas mixture. The inspired oxygen fraction (FiO₂) was set to 0.4, and the inspiratory pressure and the respiration rate set to give an arterial CO₂ (PaCO₂) of approximately 35 mmHg.

A catheter was inserted into the right common carotid artery and advanced so that the tip was located close to the aorta. This catheter was used for the collection of arterial blood samples and to measure mean arterial blood pressure and heart rate using a strain gauge transducer. A second catheter was inserted in the same carotid artery but advanced towards the base of the brain and saline infused at a rate of 1 ml h⁻¹. This was performed so that the accuracy of this methodology can be determined for experimental protocols in which substances are infused directly into the circle of Willis. Finally, the artery was tied between the catheters so that there was no blood flow to the brain via the right carotid artery. A 3.5 French catheter was sited in the right jugular vein and advanced towards the heart until the tip was sited close to the vena cava and used for the bolus injection of ICG. A third catheter was sited in the umbilical vein for infusion of 10% glucose solution at 2 ml h⁻¹ to prevent hypoglycaemia.

The piglet was placed in a stereotactic frame and rested on a heated water mattress with the water temperature adjusted to maintain normal rectal temperature (38.5 °C). An area of the scalp over the anterior fontanel approximately 0.8 cm² was removed, the skull thinned with a burr and a catheter was sited in the sagittal sinus for the collection of venous blood samples. The bone was then sealed with cyanoacrylate glue and the NIR optodes were positioned and held firmly against the scalp about 2 cm apart across the midline 1 cm anterior to the centre suture. As previously (Springett *et al* 2000b), the optodes were surrounded by NIR opaque sponges and the cranium painted with NIR opaque paint to shield the optodes from the room lights. The paint and sponges ensure that light emerging near the transmit optode did not re-enter the head near the receive optode and interfere with the attenuation measurement.

The near-infrared system has been described previously (Springett *et al* 2000a). In brief, light from a tungsten halogen lamp was transmitted to the piglet's head with a fibre bundle of diameter 3.3 mm and the transmitted light was collected with another fibre bundle and focused onto the slits of an imaging spectrograph which dispersed the light onto a cooled charge-coupled

device (CCD) detector. Complete attenuation spectra between 680 and 1000 nm were collected contiguously with a period of 50 ms, a pixel bandpass of 0.32 nm and spectral resolution of 5 nm. In this study the maximum signal was typically 70 000 electrons per digital conversion. Changes in the cerebral concentration of ICG were measured by fitting the specific absorption of ICG, oxyhaemoglobin (HbO₂), deoxyhaemoglobin (Hb) and cytochrome oxidase (Cyt), which had been corrected for the wavelength dependence of the differential pathlength, to changes in attenuation between 780 and 900 nm. The differential pathlength was determined from the 840 nm water-feature using the second-differential technique assuming a water content of 85% (Matcher *et al* 1994). The specific absorption spectrum of ICG was obtained by measuring the attenuation spectrum of ICG dissolved in human blood plasma at a temperature of 36.5 °C.

Arterial and venous blood samples were analysed for haemoglobin content and saturation with a co-oximeter calibrated for pig blood (OSM3, Radiometer, Copenhagen), for blood gases (ABL505, Radiometer, Copenhagen, Denmark) and for glucose and lactate concentration (2300 STAT Plus, YSI Inc., Yellow Springs, Ohio, USA). CMRO₂ was calculated from

$$\text{CMRO}_2 = \text{CBF} \times C_a\text{Hb} \times (\% \text{Hb}_a - \% \text{Hb}_v) \quad (3)$$

where $C_a\text{Hb}$ is the baseline arterial haemoglobin content and $\% \text{Hb}_a$ and $\% \text{Hb}_v$ are the percentage of arterial and venous (sagittal sinus) blood that is oxygenated: the values were not corrected for the oxygen dissolved in the plasma. Values of CBF and CMRO₂ were converted from units per litre of tissue to per 100 g of tissue assuming a tissue density of 1.05 g ml⁻¹.

ICG (Pulsion Medical Systems, Munich, Germany) was freshly dissolved in sterile water to a concentration of 1 mg ml⁻¹ prior to each study. Before the beginning of the study the catheter sited in the jugular vein was primed with ICG solution so that a bolus of $\approx 80 \mu\text{l}$ could be injected from a 1 ml syringe over a period of ≈ 0.3 s when required. No saline flush was necessary because the dead space of the catheter was always filled with ICG solution and because there was a continuous flow of blood past the tip of the catheter. This procedure ensured that a sharp bolus of ICG could be introduced with minimal fluid loading. Although the bolus could be injected more rapidly, carefully analysis of the heart rate trace for rapid injections showed small transient perturbations at the time of the injection, probably as a result of the sudden increased pressure in the vena cava.

The arterial concentration was obtained from a Nihon Koden dye densitogram analyser (model DDG-2001) with the probe positioned on the left front foot. This instrument provides an arterial concentration every heartbeat, which in this study was approximately every 0.4 s. This data was then interpolated to the same frequency as the NIR data (0.05 s) and time-registered to the tissue curve (see section 3). For the differential method, the tissue ICG signal was numerically differentiated using a Savitzky–Golay algorithm described by Press *et al* (1992), using a fourth-order polynomial and a half width of 20 data points (1 s) to give $C'_t(t)$. The arterial curve was also smoothed using a Savitzky–Golay algorithm with the same parameters before performing the regression to compensate for the small but inevitable broadening of the tissue ICG curve caused by the differential algorithm.

At the end of the preparation the isoflurane was reduced to 1.8% and the piglet was allowed to stabilize for at least 1 h. Each measurement of CMRO₂ and CBF consisted of withdrawal of 0.25 ml of blood from the catheter sited in the sagittal sinus followed by 0.25 ml from the catheter sited close to the aorta and then the bolus injection of ICG.

The experimental protocol consisted of four measurements of CBF and CMRO₂, at baseline, at two levels of hypercapnia induced by increasing the inspired CO₂ fraction (FiCO₂) to 0.03 and then 0.06, and then again at normocapnia. Fifteen minutes were allowed between increasing FiCO₂ and the collection of blood samples and bolus injection because the

Table 1. Physiological parameters measured before each blood flow expressed as mean \pm SD ($n = 7$) at different inspired CO₂ fractions. MAP is mean arterial blood pressure, PaO₂ is arterial oxygen tension and PaCO₂ is arterial CO₂ tension. ** $P < 0.005$, * $P < 0.05$ from baseline using a paired Student's t -test.

| | Baseline, FiCO ₂ = 0.0 | Hypercapnia 1, FiCO ₂ = 0.03 | Hypercapnia 2, FiCO ₂ = 0.06 | Normocapnia 2, FiCO ₂ = 0.0 |
|--|--------------------------------------|--|--|---|
| MAP (mmHg) | 50.9 \pm 4.4 | 51.4 \pm 3.4 | 53.5 \pm 3.8* | 50.2 \pm 3.9 |
| Heart rate (beats min ⁻¹) | 155 \pm 8 | 155 \pm 8 | 162 \pm 10* | 160 \pm 9* |
| Temperature (°C) | 38.6 \pm 0.1 | 38.6 \pm 0.1 | 38.5 \pm 0.1 | 38.6 \pm 0.1 |
| PaO ₂ (mmHg) | 121.4 \pm 35.1 | 130.4 \pm 29.6 | 117.1 \pm 25.8 | 134.9 \pm 34.2 |
| PaCO ₂ (mmHg) | 33.0 \pm 2.2 | 42.1 \pm 2.6** | 54.2 \pm 3.1** | 34.5 \pm 2.4 |
| Arterial pH (pH units) | 7.55 \pm 0.03 | 7.46 \pm 0.02** | 7.38 \pm 0.02** | 7.55 \pm 0.04 |
| Arterial glucose (mM) | 5.1 \pm 0.4 | 5.2 \pm 0.5 | 5.2 \pm 0.5 | 5.2 \pm 0.6 |
| Arterial lactate (mM) | 1.8 \pm 0.7 | 1.6 \pm 0.5 | 1.2 \pm 0.3* | 1.4 \pm 0.2 |

haemoglobin signals from the NIR system showed that cerebral haemodynamics were stable at this time, and 30 min were allowed when FiCO₂ was switched back to zero for the final measurement. The inspired oxygen fraction was maintained at 0.40 throughout and the balance was nitrogen.

Results are expressed as mean \pm SD ($n = 7$) and the statistical significance of changes were determined with a paired Student's t -test.

3. Results

Table 1 shows physiological values averaged for all animals prior to the measurement of blood flow at baseline, the two levels of hypercapnia and finally at normocapnia. Heart rate, mean arterial pressure and rectal temperature were in the normal range for a newborn piglet. Increasing FiCO₂ led to an increase in PaCO₂ and a decrease arterial pH in well-defined and highly significant steps as expected and these parameters returned to their baseline values once FiCO₂ was returned to zero. Arterial glucose and lactate concentrations were in the normal range and the glucose concentration did not change significantly whereas the lactate concentration showed a small but almost continuous decline throughout the study, probably as part of the recovery from the surgery.

Figure 1 showed the arterial and tissue ICG signals from a baseline measurement in a single piglet. Time zero is chosen as the point at which the arterial concentration begins to increase. The arterial concentration (figure 1(a)), measured from the ICG pulse oximeter, confirms that the method for injection ICG produces a sharp bolus. The bolus has a peak at ≈ 1.81 s which then falls almost to baseline then rises to a steady state of ≈ 16 s as the ICG is evenly distributed throughout the vasculature of the whole body. In these piglets, the plasma half-life is approximately 20 min as indicated by the slow return of the tissue signal to baseline. The rising half-width half-maximum of the arterial bolus was 0.9 s and the full-width half-maximum was 3.22 s. The tissue curve measured with the NIR system is similarly bolus

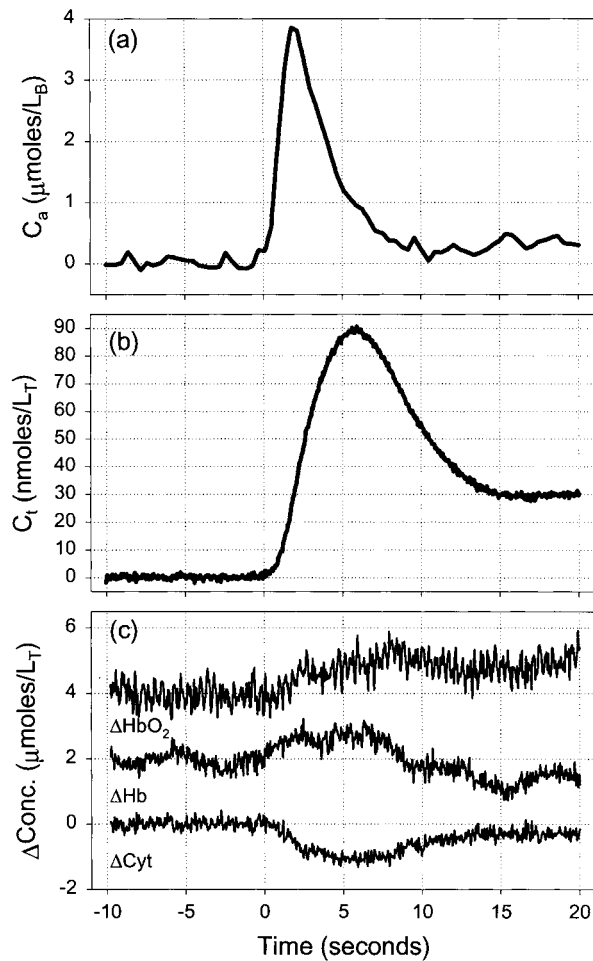


Figure 1. Typical (a) arterial (C_a) and (b) tissue (C_t) ICG concentration curves obtained at normocapnia from a typical piglet and (c) simultaneous changes in the NIRS signals. ΔHbO_2 is oxyhaemoglobin, ΔHb is deoxyhaemoglobin and ΔCyt is cytochrome oxidase. The NIRS signals have been offset by $2 \mu\text{mol l}^{-1}$ for clarity. The subscripts B and T on the concentration unit refer to blood and tissue respectively.

shaped but broader with a peak at 5.6 s. The peak in the tissue concentration appears when ICG inflow is equal to the outflow (equation (1)) and occurs before the arterial bolus has completely entered the field of view.

Figure 1(c) shows the changes in concentration of the other chromophores included in the fitting algorithm and gives an indication of the degree of crosstalk between the signals. Each trace has been offset by $2 \mu\text{mol l}^{-1}$ for clarity. The higher apparent noise on the ΔHbO_2 trace is actually the pulseatile component from the heartbeat. In addition, the ΔHbO_2 and ΔHb traces show variations with the breathing frequency (period ≈ 5 s) and other lower-frequency components which have been associated with vasomotion (Elwell *et al* 1999) which are at least of a similar magnitude to the crosstalk. The cytochrome signal is more stable in the baseline period than the haemoglobin signals and clearly shows a pronounced reduction that mirrors the shape of the ICG curve. The most likely cause of this reduction is crosstalk.

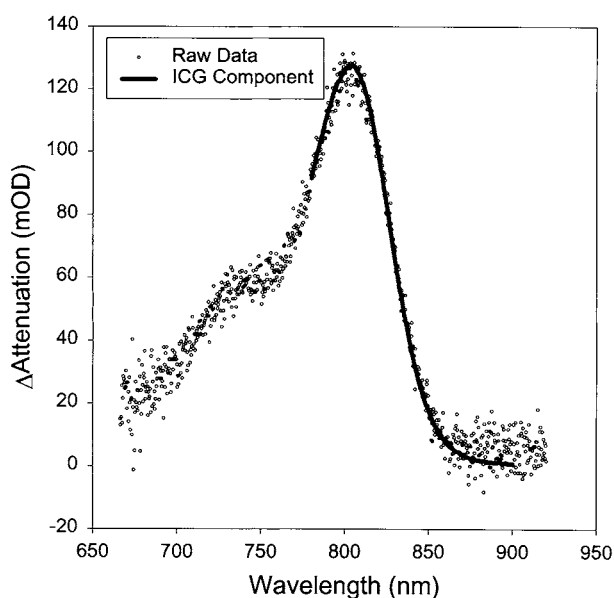


Figure 2. Comparison of the measured change in attenuation spectrum and the ICG component of the least squares fit. The time point was obtained at the maximum of the tissue concentration from figure 1.

Figure 2 shows the change in the attenuation spectrum obtained at the maximum of the tissue ICG curve and is an indication of the signal to noise which can be obtained with this system in this model using an integration time of 50 ms. The bold curve on figure 2 is the component of the attenuation spectrum that the fitting algorithm attributes to ICG. Although crosstalk between the cerebral ICG concentration and other components is clearly apparent in figure 1 and the attenuation of the other components is not insubstantial (≈ 10 mOD), the changes are in part equal and opposite so that the component of the attenuation spectrum which cannot be accounted for by ICG is very small.

Figure 3 shows how CBF is calculated from the data in figure 1 with the integral method in the two panels and the differential method in the bottom panels. In figure 3(a), the integral of the arterial concentration is shown plotted along with the tissue curve scaled by the calculated blood flow. Figure 3(b) shows the same data plotted with the integral of the arterial function on the x -axis and the tissue curve on the y -axis. With increasing time (shown by the arrow) the curve in figure 3(b) starts at the origin and increases linearly as the ICG washes into the brain. The ICG begins to wash out before the end of the bolus and the curve becomes sublinear and then falls rapidly as outflow exceeds inflow. Finally the traces reaches a stable level when the bolus has completely passed through the body and has evenly distributed itself throughout the vasculature. At this point the concentration within the field of view is constant and outflow is equal to inflow. The gradient of the linear portion gives the blood flow and in this case it is $47.1 \text{ ml } 100 \text{ g}^{-1} \text{ min}^{-1}$.

Figure 3(c) compares the arterial signal with the differential of the tissue signal normalized to the blood flow. The same data are plotted in figure 3(d) with the arterial signal plotted on the x -axis and the differential of the tissue signal on the yu -axis. With increasing time (shown by arrows) the curve in figure 3(d) starts at the origin, increases linearly until the peak of the bolus and then decreases along nearly the same line until the washout begins whereupon the data fall

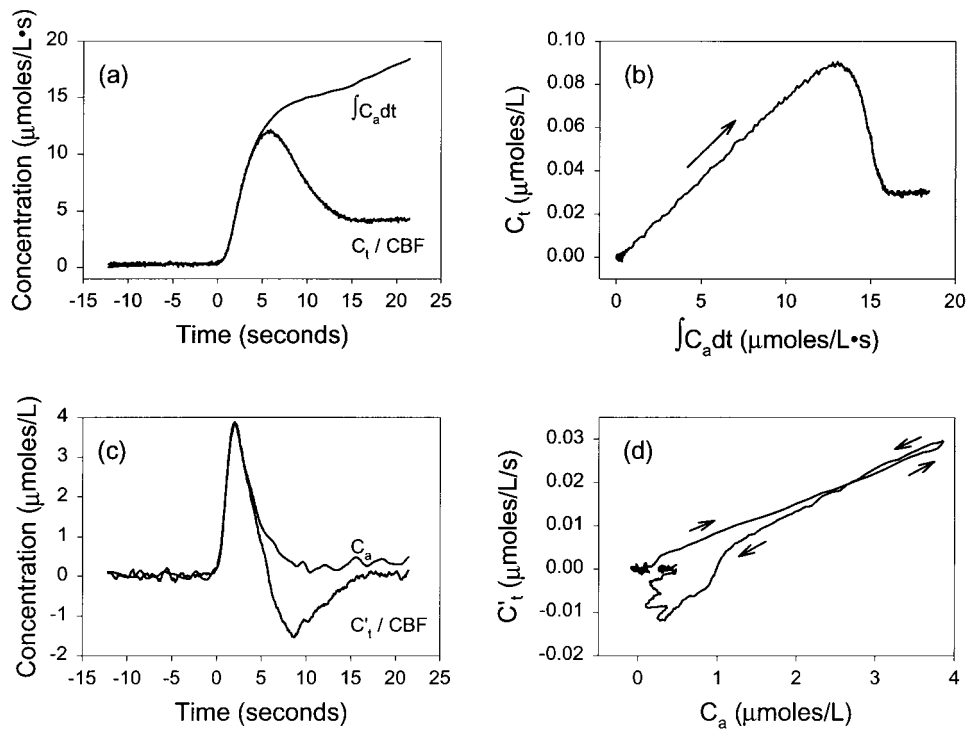


Figure 3. Graphical representation of the analysis techniques. Integral method: the integral of the arterial concentration and the tissue concentration scaled by the calculated blood flow plotted against time (a) and the relationship between the two (b). Differential method: the arterial concentration and time differential of the tissue concentration scaled by the calculated blood flow plotted against time (c) and the relationship between the two (d). The arrows show increasing time.

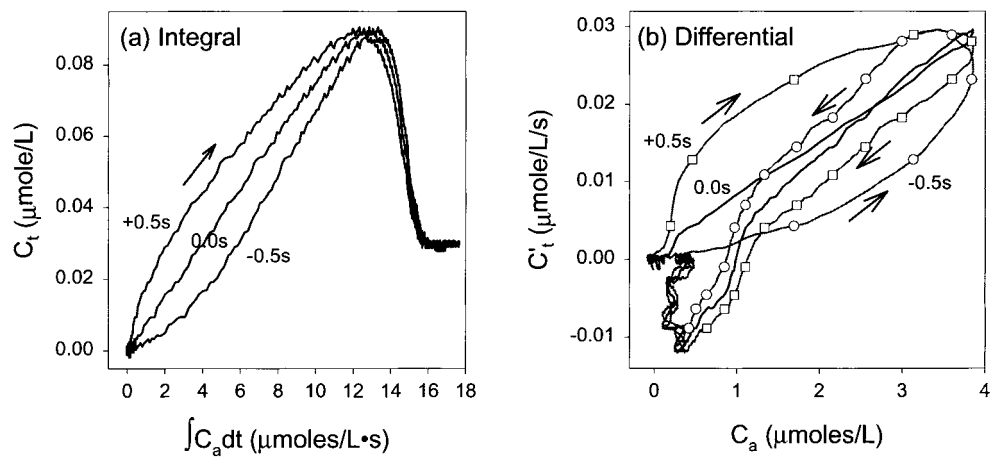


Figure 4. Effects of misregistration on the regression for (a) the integral method and (b) the differential method. The arrows show increasing time.

below the line. The gradient of linear portion included all the data until washout begins gives the blood flow and in this case is $46.7 \text{ ml } 100 \text{ g}^{-1} \text{ min}^{-1}$.

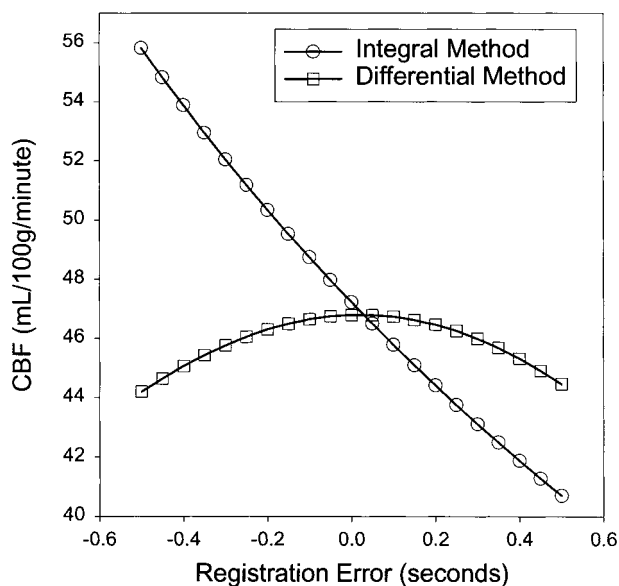


Figure 5. Blood flow values obtained as a function of misregistration from the integral and differential technique.

Figure 4(a) shows the effects of time registration on the relationship between the integral of the arterial concentration and the tissue signal. For correct registration (0.0 s), the relationship is linear until washout commences. When the arterial signal is shifted forward in time by 0.5 s with respect to the tissue signal then the relationship becomes nonlinear with a gradient that is initially too steep but then decreases to a stable value before washout.

Similarly, when the arterial curve is shifted back in time by 0.5 s, the initial gradient is too shallow but then increases towards the point at which washout begins. Manual registration was achieved by varying the registration in steps of 0.05 s and determining when the relationship shown in figure 4 becomes the closest to linear. Figure 4(b) shows similar data for the differential method but in this case the interpretation is more complicated. When the arterial signal is shifted in time with respect to the tissue signal, the downswing does not follow the upswing but instead the relationship becomes a loop. The effects of misregistration on the calculated blood flow for the integral and differential method was presented in figure 5. In the case of the integral method, the relationship between registration and calculated blood flow is almost linear with a gradient of $15 \text{ ml } 100 \text{ g}^{-1} \text{ min}^{-1} \text{ s}^{-1}$ so that even small errors in registration lead to substantial errors in the calculated blood flow, e.g. a 0.1 s misregistration will lead to an error of $\approx 3\%$ in the calculated blood flow. In contrast, the relationship for the differential method shows a maximum at the correct registration point and so this method is much less sensitive to errors in registration. Although the integral and differential technique produce essentially the same value for blood flows when the curves are accurately time-registered, the differential method is less sensitive to errors in time registration and so is used to calculate the values of blood flow presented in table 3 and figures 7 and 8.

Figure 6 compares the bolus curves at normocapnia and at the highest level of hypercapnia in a typical piglet. The calculated values of blood flow are 46.7 and $78.0 \text{ ml } 100 \text{ g}^{-1} \text{ min}^{-1}$ at normocapnia and hypercapnia respectively. From this figure it can be seen that the effect of hypercapnia on the arterial signal is negligible with the same peak concentration and rise

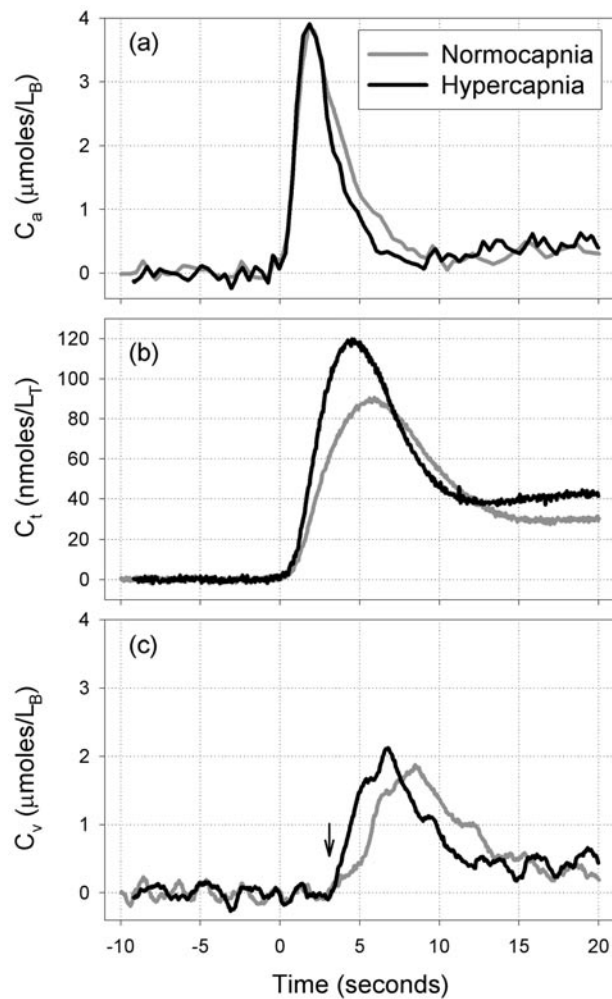


Figure 6. Comparison of (a) the arterial concentration, (b) the tissue concentration and (c) the calculated venous concentration of ICG between baseline ($\text{FiO}_2 = 0.00$) and hypercapnia ($\text{FiCO}_2 = 0.06$). The subscripts B and T on the concentration unit refer to blood and tissue respectively.

time but a small change in the bolus width. However, the tissue concentrations are very different with a sharper rise during hypercapnia and reaching a higher concentration, as would be expected because the higher blood flow increases the rate at which ICG enters the field of view. The venous outflow is shown in figure 6(c), where it can be seen that the distribution of transit times shifts to a shorter time during hypercapnia compared to normocapnia. The minimum transit time (marked with an arrow) in this piglet is approximately 3.4 s, at which point the majority of the bolus has entered the field of view. Note that, similar to the arterial inflow, the venous outflow does not return to baseline.

Table 2 shows the NIR parameters collected immediately before each measurement of blood flow. As has been described previously (Springett *et al* 2000b), hypercapnia results in large increases in HbO_2 and HbT but only small decreases in Hb . These large increases in haemoglobin concentration and saturation result in a large increases in the tissue absorption

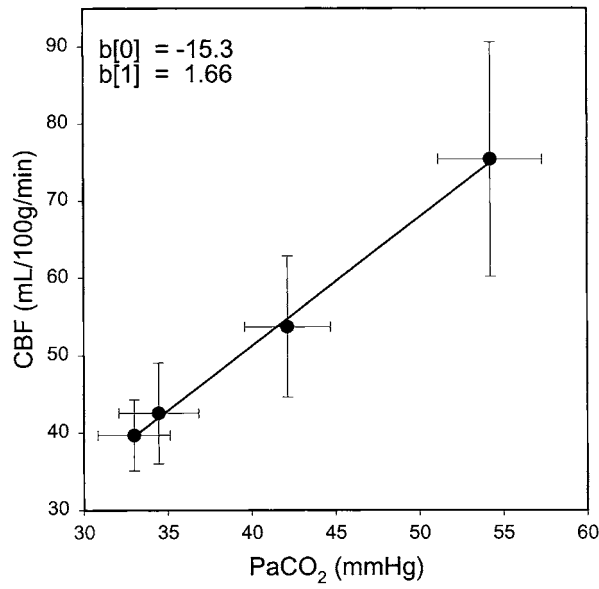


Figure 7. The response of CBF to hypercapnia calculated using the differential method. The points are mean ± SD ($n = 7$) and the linear regression line is a guide for the eye.

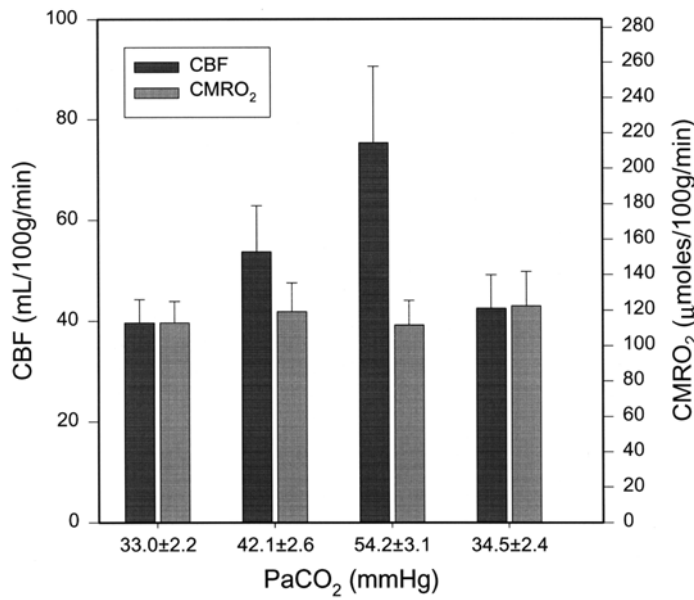


Figure 8. The response of CBF and CMRO₂ to hypercapnia plotted as a bar chart. The CMRO₂ axis has been chosen so that the baseline ($PaCO_2 = 33.0 \pm 2.2$) bar heights are the same. Results are plotted as mean ± SD ($n = 7$).

coefficient and a decrease in the differential pathlength of approximately 9% at the highest level of hypercapnia. If the chromophore concentrations are not corrected for the change in differential pathlength, then the calculated blood flow and oxygen consumption will be systematically underestimated by 9%.

Table 2. Changes in cerebral oxyhaemoglobin (ΔHbO_2), deoxyhaemoglobin (ΔHb) and total haemoglobin (ΔHbT) from baseline and differential pathlength measured before each blood flow at different levels of arterial CO_2 tension ($P\text{aCO}_2$). Results are expressed as mean \pm SD ($n = 7$). ** $P < 0.005$, * $P < 0.05$ from baseline using a paired Student's t -test.

| | Baseline, $P\text{aCO}_2 =$ 33.0 ± 2.2 mmHg | Hypercapnia 1, $P\text{aCO}_2 =$ 42.1 ± 2.6 mmHg | Hypercapnia 2, $P\text{aCO}_2 =$ 54.2 ± 3.1 mmHg | Normocapnia 2, $P\text{aCO}_2 =$ 34.5 ± 2.4 mmHg |
|--|---|--|--|--|
| ΔHbO_2 ($\mu\text{mol l}^{-1}$) | 0 | $9.6 \pm 2.3^{**}$ | $23.4 \pm 6.4^{**}$ | -0.6 ± 4.0 |
| ΔHb ($\mu\text{mol l}^{-1}$) | 0 | $-0.9 \pm 1.9^{**}$ | $-2.3 \pm 1.8^{**}$ | 0.3 ± 0.8 |
| ΔHbT ($\mu\text{mol l}^{-1}$) | 0 | $8.7 \pm 2.4^{**}$ | $21.0 \pm 6.4^{**}$ | -0.4 ± 3.9 |
| Pathlength (cm) | 8.1 ± 0.7 | $7.7 \pm 0.6^{**}$ | $7.4 \pm 0.6^{**}$ | 8.0 ± 0.7 |

The relationship between $P\text{aCO}_2$ and CBF (calculated with the differential method) is shown in figure 7 and, as expected, is linear over this range of $P\text{aCO}_2$ with a gradient of $166 \text{ ml } 100 \text{ g}^{-1} \text{ min}^{-1} \text{ mmHg}^{-1}$. These results are also shown in table 3 along with arterial and venous oxygen content and oxygen consumption. Oxygen content is expressed as the per cent of total haemoglobin that has bound oxygen. The co-oximeter recorded a combined methaemoglobin and carboxyhaemoglobin content of approximately 2% of the total haemoglobin and therefore the arterial and venous saturation (defined in terms of the functional haemoglobin) was approximately 2% and 1% higher respectively than the values shown in table 3.

Figure 8 is a bar graph showing CBF and CMRO_2 values from table 3 at the four levels of $P\text{aCO}_2$. For comparison, the CMRO_2 axis has been scaled so that the baseline bar heights are the same. With increasing $P\text{aCO}_2$, CBF increased and venous saturation also increased, resulting in a decreasing arterial–venous difference in proportion to the increase in CBF. This resulted in a value of CMRO_2 that was not significantly different from baseline even though CBF had increased by about 90% at the highest level of hypercapnia. The 9% increase in mean CMRO_2 between normocapnic baseline and normocapnia post hypercapnia was not significant ($P > 0.07$).

4. Discussion

In this piglet model one carotid artery is totally occluded and blood reaches the circle of Willis via the remaining carotid artery and the vertebral arteries. Although each carotid artery usually carries about 40% of the blood flow to the brain, it is well known that, apart from transitory effects, one artery can be occluded without changing blood flow to the brain or the blood flow response to hypercapnia.

One assumption in the application of the Fick principle to this methodology is that the measured arterial concentration is the same as the arterial concentration that is feeding the field of view of the NIR system. For this reason, the left front foot was chosen to monitor the arterial function because the subclavian arteries (which feed the front feet), as well as the common carotid and vertebral arteries, leave the aortic arch before the ductus arteriosus whereas the back feet are post ductal. Although there was no evidence that the duct was patent, the physiology of the duct would suggest that some leakage is possible immediately after birth. More importantly, multiple routes of blood flow from the aorta to the field of view

Table 3. Blood flow and oxygen consumption parameters expressed as mean \pm SD ($n = 7$). P_{aCO_2} is arterial CO_2 tension, CaHb is arterial haemoglobin content, HbO_2 is the percentage of haemoglobin that is oxygenated and $CMRO_2$ is cerebral metabolic rate for oxygen. ** $P < 0.005$, * $P < 0.05$ from baseline using a paired Student's t -test.

| | Baseline, $P_{aCO_2} =$ 33.0 \pm 2.2 mmHg | Hypercapnia 1, $P_{aCO_2} =$ 42.1 \pm 2.6 mmHg | Hypercapnia 2, $P_{aCO_2} =$ 54.2 \pm 3.1 mmHg | Normocapnia 2, $P_{aCO_2} =$ 34.5 \pm 2.4 mmHg |
|---|---|--|--|--|
| CBF (ml 100 g ⁻¹ min ⁻¹) | 39.7 \pm 4.6 | 53.7 \pm 9.1** | 75.4 \pm 15.2** | 42.6 \pm 6.6 |
| CaHb (g l ⁻¹) | 92.4 \pm 11.7 | 92.7 \pm 13.1 | 92.3 \pm 11.8 | 92.6 \pm 10.3 |
| Arterial HbO_2 (%) | 96.3 \pm 1.0 | 96.1 \pm 2.2 | 96.1 \pm 1.3 | 97.0 \pm 0.4 |
| Venous HbO_2 (%) | 45.6 \pm 5.9 | 56.6 \pm 3.4** | 69.5 \pm 2.6** | 45.7 \pm 6.6 |
| $CMRO_2$ (μ mol 100 g ⁻¹ min ⁻¹) | 113 \pm 12 | 119 \pm 16 | 112 \pm 14 | 122 \pm 19 |

would lead to dispersion in the arterial bolus and broadening of the arterial inflow. This would be apparent in figures 1 and 6 because the differential of the tissue concentration, which is equal to the difference between inflow and outflow into the field of view (equation (2)), would be broader than the arterial bolus. In some of the measured blood flows, the arterial signal was slightly broader than the differential of the tissue concentration and this was more prevalent at normocapnia when blood flow was lower than at hypercapnia. The observation of little dispersion in the arterial function and a minimum transit time of several seconds gives some information on the sensitivity of the NIR system to different parts of the vasculature. If the NIR system only probed the capillary bed then the minimum transit time would be very short and substantial dispersion would be expected from the multiple anastomoses that are observed at the level of very small vessels. Therefore, these data provide experimental evidence that NIR systems are sensitive to the penetrating arterioles and venules and probably the smaller pial arteries and veins, in agreement with modelling (Firbank *et al* 1997).

As expected, the venous outflow is broader than the arterial inflow because the bolus has passed through the capillary bed that has multiple transit times. During hypercapnia when blood flow has increased and the increase in total haemoglobin would indicate that there has been an increase in cerebral blood volume, it can be seen that the distribution of venous outflow shifts to shorter times and becomes narrower (figure 3). This is in agreement with the observations from the tracking of labelled red blood cells through the capillary bed with video microscopy that the distribution of transit times becomes shorter and more homogeneous (Hudetz 1997).

Once the venous outflow has been calculated it should be possible to measure the mean transit time (MTT) which can be calculated from

$$MTT = \left(\int_0^{\infty} t(C_a(t) - C_v(t)) dt \right) \left(\int_0^{\infty} C_a(t) dt \right)^{-1} \quad (4)$$

and then cerebral blood volume can be obtained via the central volume theorem. In this case, a mean transit time cannot be calculated because the arterial ICG concentration does not return to zero after passage of the bolus due to recirculation of tracer and redistribution throughout the whole vasculature of the body. As can be seen from figure 3(a), the denominator of equation (3) does not converge in a finite time and there is no obvious point at which the integral can be truncated.

Accurate calculation of blood flow requires the accurate measurement of the tissue ICG concentration, which is difficult to validate independently. Previously this full-spectral NIR system has been shown to accurately separate the small cytochrome oxidase signal in the presence of much larger changes in haemoglobin (Springett *et al* 2000a, b). The change in attenuation as a result of the bolus of ICG is much larger than concurrent changes in haemoglobin (see figure 2) and, although crosstalk between the cerebral ICG concentration and the cytochrome signal can be observed (see figure 1), the difference in the observed attenuation change and the component that the fitting algorithm attributes to ICG is small. This is evidence that the ICG signal has been accurately separated from the other chromophores. The error in the cytochrome signal is approximately 50% of the total cytochrome oxidase content of the newborn piglet brain (Springett *et al* 2000b) and so it must be concluded that, currently, the cytochrome signal cannot be used as an indicator of cytochrome oxidase redox state in the presence of ICG.

Once the attenuation spectrum has been split into the individual chromophore components it is necessary to normalize the components to the differential pathlength in order to produce concentrations in absolute units (e.g. nmol l⁻¹). In contrast to other intensity-based NIR systems which estimate the differential pathlength as a multiple of the optode separation, the full-spectral NIR system is able to measure the differential pathlength from the water absorption feature at 840 nm using a second-differential analysis and assuming a certain concentration of water. Hypercapnia increases the cerebral haemoglobin concentration and hence increases the tissue absorption coefficient. The increase in tissue absorption coefficient decreases the differential pathlength (see table 2) even though optode separation has not changed. This change cannot be accounted for in traditional intensity-based NIR systems and would lead to a consistent 9% underestimation of both CBF and CMRO₂. This would make the changes in CMRO₂ during hypercapnia statically significant and therefore it is essential to measure the differential pathlength before an accurate measurement of CBF can be made.

Figure 5 clearly shows that accurate time registration between the arterial and tissue curve is essential for the correct measurement of CBF. Unlike the fiberoptic catheter (Pulsion) system used previously (Patel *et al* 1998, Roberts *et al* 1998), the Nihon Koden pulse oximeter does not provide a continuous output of arterial ICG concentration and so it is not possible to automatically synchronize the tissue curve with the arterial curve. Instead, the arterial data are downloaded from the pulse oximeter after the bolus injection and the data must be registered manually. Even if synchronization were possible, there would still be a significant time delay from blood leaving the heart before it arrives within the field of view of the NIRS optodes and this would mean that registration would still be necessary given the sensitivity of the calculated blood flow to errors in registration.

Roberts *et al* (1998) observed that their value of blood flow depended on the exact integration period that they used to calculate the blood flow and explained this in terms of inhomogeneity of blood flow. In general, two flow components can be observed with techniques that measure the outflow of a diffusable tracer over a period of several minutes. The fast component is attributed to grey matter and the slow component to white matter. Two components are observable because at early times the fast compartment dominates the outflow, whereas at later times the concentration of the fast compartment has fallen to zero and the remaining outflow is from the slow compartment. Flow inhomogeneity cannot be observed in an inflow technique because inflow is simultaneous in both compartments. The tissue concentration of tracer is then the sum from both components and the resulting blood flow is an average weighted by the relative volume and sensitivity of the NIRS system to each compartment. If inflow were not simultaneous in both compartments then a linear relationship between the integral of the arterial concentration and the tissue concentration could not be

obtained by varying the registration between the signals. The most likely cause of this variation in calculated blood flow with integration period is misregistration: if the arterial curve were delayed with respect to the tissue curve (positive misregistration in figure 4), the blood flow calculated with the two-point method would initially overestimate blood flow and then converge towards a constant value. For correct registration, the gradient of the tissue concentration plotted against the integral of the arterial concentration is independent of integration time until washout begins.

Light distribution modelling has shown that placement of the NIR optodes 2 cm apart across the midline should produce a banana-shaped region of highest sensitivity that is approximately 1 cm deep (Arridge and Schweiger 1995). The skin and skull layer in newborn piglets is extremely thin (2–3 mm) which should ensure that dilution of the field of view by extracerebral tissue is extremely small and accurate values of tissue tracer concentration and hence blood flow are measured. It is generally accepted that the sagittal sinus drains mainly cortical blood and therefore it is valid to use this CBF value along with arterial sagittal sinus saturation differences to calculate $CMRO_2$ of the cortex. It has previously been shown that CBF is highly dependent on $PaCO_2$ whereas $CMRO_2$ is independent of $PaCO_2$ over the range from normocapnia to mild hypercapnia presented here. If it is accepted that hypercapnia does not affect $CMRO_2$ then $CMRO_2$ can be used to validate the blood flow value if arterial and venous saturation are measured reliably because venous saturation must increase in order to maintain $CMRO_2$ constant at increased CBF (equation (3)). In this study, arterial and venous saturation was measured with a six-wavelength co-oximeter calibrated for pig blood, which is considered to be a gold standard. By reproducing these finds we have validated the ICG blood flow technique but only to within an arbitrary scaling factor. Although this scaling factor could be different for each piglet, this CBF method can be used to measure changes in $CMRO_2$ from baseline.

The baseline blood flow of 53.7 ± 9.1 ml 100 g $^{-1}$ min $^{-1}$ at $PaCO_2$ of 42 mmHg is comparable to some literature values of blood flow in the newborn piglet but not others. For example, Bauer *et al* (1999) measured a value of 56 and 43 ml 100 g $^{-1}$ min $^{-1}$ in cerebral cortex and white matter respectively at a $PaCO_2$ of 39 mmHg in piglets anaesthetized with isoflurane whereas DeGiulio *et al* (1989) measured 78 and 35 ml 100 g $^{-1}$ min $^{-1}$ in cerebral grey and white matter at a $PaCO_2$ of 37 mmHg using halothane and Goldstein *et al* (2000) measured a cortical flow of 89 ml 100 g $^{-1}$ min $^{-1}$ in conscious piglets at a $PaCO_2$ of 43 mmHg. All these measurements were made using microspheres from piglets in the first few days of life. The substantial difference between blood flow in the white and grey matter would complicate a direct validation using microspheres because the ratio of white to grey matter in the field of view it is not known. Even with other recognized blood flow techniques, it is accepted that different laboratories can produce slightly different baseline values from the same model and under the same anaesthetic regime (Siesjo 1978).

Although this data set was not designed to measure the intrasubject variability of the method, some measure can be determined by comparing the blood flow values at baseline and normocapnia post hypercapnia. Although a hypercapnic swing and approximately an hour in time separate these measurement points the difference in the blood flow between these two measurements was only 2.9 ± 3.0 ml 100 g $^{-1}$ min $^{-1}$ over a period when $PaCO_2$ had increased by 1.5 ± 3.4 mmHg. From figure 7 it can be seen that this increase in mean blood flow can be almost fully accounted for by the increase in mean $PaCO_2$ because this data point falls on the regression line. The standard deviation of the change, which is 7% of the mean, gives an estimation of the variance in the measurement and is evidence that this techniques of cerebral blood flow is extremely precise.

The overall aim of this research is to develop a technique to make multiple measurements of CBF in a piglet model to allow the measurement of oxygen consumption using arterial and

venous blood samples. Currently, the microsphere technique is typically limited to six measurements because, in general, only six different types of microspheres are available (e.g. different radioisotopes or different colours) and the animal must be sacrificed at the end of the study in order to calculate CBF. In contrast, because the plasma half-life of ICG is only 20 min, blood flow could be measured repeatedly over long period of times. This could be particularly useful for a hypoxic–ischaemic insult/secondary energy failure model; (Lorel *et al* 1994) in which the piglet remains anaesthetized for 48 h during the onset of secondary energy failure. Alternatively, because the ICG technique is minimally invasive, if necessary the animal can be recovered from anaesthesia at the end of a study and can then be measured again on a different day.

In summary, the ICG bolus technique has been examined and it has been shown that the blood flow calculated using the integral method is extremely sensitive to the time registration between the arterial and tissue signals. The differential method is more robust with respect to time registration and is also able to give the venous outflow. The differential method has been shown to be extremely precise and the accuracy has been partially validated against oxygen consumption during a hypercapnic challenge.

Acknowledgments

We are grateful to Hamamatsu Phototonic KK for financial assistance.

References

- Arridge S R and Schweiger M 1995 Photon-measurement density functions. Part 2: Finite-element-method calculations *Appl. Opt.* **34** 8026–37
- Bauer R, Bergmann R, Walter, B Brust P, Zwiener U and Johannsen B 1999 Regional distribution of cerebral blood volume and cerebral blood flow in newborn piglets—effect of hypoxia/hypercapnia *Brain Res. Dev. Brain Res.* **112** 89–98
- DeGiulio P A, Roth R A, Mishra O P, Delivoria-Papadopoulos M and Wagerle L C 1989 Effect of indomethacin on the regulation of cerebral blood flow during respiratory alkalosis in newborn piglets *Pediatr. Res.* **26** 593–7
- Elwell C E, Cope M and Delpy D T 1997 An analytical method for determining cerebrovascular transit time using near infrared spectroscopy *Adv. Exp. Med. Biol.* **471** 57–65
- Elwell C E, Springett R, Hillman E and Delpy D T 1999 Oscillations in cerebral haemodynamics. Implications for functional activation studies *Adv. Exp. Med. Biol.* **471** 57–65
- Firbank M, Okada E and Delpy D T 1997 Investigation of the effect of discrete absorbers upon the measurement of blood volume with near-infrared spectroscopy *Phys. Med. Biol.* **42** 465–77
- Goldstein M, Rehan V K, Oh W and Stonestreet B S 2000 Cerebral and intestinal perfusion and metabolism in normocytic hyperviscous hypoxic newborn pigs *J. Appl. Phys.* **88** 2107–15
- Hudetz A G 1997 Regulation of oxygen supply in the cerebral circulation *Adv. Exp. Med. Biol.* **428** 513–20
- Kuebler W M, Sckell A, Habler O, Kleen M, Kuhnle G E H, Welte M, Messmer K and Goetz A E 1998 Noninvasive measurement of regional cerebral blood flow by near infrared spectroscopy and indocyanine green *J. Cereb. Blood Flow Metabol.* **18** 445–56
- Lassen N A 1984 Cerebral transit of an intravascular tracer may allow measurement of regional blood volume but not regional blood flow *J. Cereb. Blood Flow Metabol.* **4** 633–4
- Lorek A *et al* 1994 Delayed (secondary) cerebral energy failure after acute hypoxia–ischemia in the newborn piglet: continuous 48-hour studies by phosphorus magnetic resonance spectroscopy *Pediatr. Res.* **36** 699–706
- Matcher S J, Cope M and Delpy D T 1994 Use of the water-absorption spectrum to quantify tissue chromophore concentration changes in near-infrared spectroscopy *Phys. Med. Biol.* **39** 177–96
- Patel J, Marks K, Roberts I, Azzopardi D and Edwards A D 1998 Measurement of cerebral blood flow in newborn infants using near infrared spectroscopy with indocyanine green *Pediatr. Res.* **43** 34–9
- Press W H, Teukolsky S A, Vetterling W T and Flannery B P 1992 *Numerical Recipes in C: the Art of Scientific Computing* (Cambridge: Cambridge University Press)
- Roberts I G, Fallon P, Kirkham F J, Kirshbom P M, Cooper C E, Elliott M J and Edwards A D 1998 Measurement of cerebral blood flow during cardiopulmonary bypass with near-infrared spectroscopy *J. Thorac. Cardiovasc. Surg.* **115** 94–102

- Siesjo B K 1978 *Brain Energy Metabolism* (New York: Wiley)
- Springett R, Newman J, Cope M and Delpy D T 2000b Oxygen dependency and precision of cytochrome oxidase signal from full spectral NIRS of the piglet brain *Am. J. Physiol. Heart Circ. Physiol.* **279** H2202–H2209
- Springett R, Wylezinska M, Cady E B, Cope M and Delpy D T 2000a Oxygen dependency of cerebral oxidative phosphorylation in newborn piglets *J. Cereb. Blood Flow Metabol.* **20** 280–9
- Weisskoff R M, Chesler D, Boxerman J L and Rosen B R 1993 Pitfalls in MR measurement of tissue blood flow with intravascular tracers: which mean transit time? *Magn. Reson. Med.* **29** 553–8